Enhanced Glaucoma Diagnosis Through U-Net Deep Learning and DenseNet-201 Feature Extraction

Syed Bacha Hussain Bukhari*, Shahzad Anwar*

* Department of Mechatronics Engineering, University of Engineering & Technology Peshawar Pakistan

Abstract- Glaucoma exhibits a significant prevalence across multiple nations, with a notable increase in prominence observed within the United States and Europe. According to recent data, the global prevalence of glaucoma stands at approximately 78 million individuals as of the year 2020. Projections indicate that this figure is expected to rise significantly to reach an estimated 111.8 million by the year 2040. In regions characterized by inadequate healthcare infrastructure aimed at addressing glaucoma, it has been observed that the condition is misdiagnosed in a staggering 90% of cases. In order to optimize the identification of early-stage glaucoma, it is crucial to develop a reliable and effective detection system. In the present study, we propose the adoption of deep learning technology as a means to detect and forecast the onset of glaucoma prior to the appearance of symptomatic indications. The utilization of a deep learning algorithm is predicated upon the utilization of a glaucoma dataset for the purpose of conducting image analysis. In order to enhance the efficacy of optic cup segmentation through the utilization of deep learning principles, the integration of pretrained transfer learning models with the U-Net architecture is seamlessly executed. In the context of feature extraction, the DenseNet-201 deep convolutional neural network (DCNN) is utilized. The utilization of the DCNN methodology plays a pivotal role in the identification and assessment of glaucoma in individuals. The principal aim of our research endeavor is to discern the presence of glaucoma in retinal fundus images, thereby enabling the evaluation of a patient's ocular health status. The bidirectional impact of glaucoma on the model results in outcomes that could vary in either a positive or negative direction. Metrics such as accuracy, recall, precision, F-measure and specificity, the F-score are of utmost importance when assessing the performance of a model. Furthermore, a comprehensive comparative analysis is undertaken in order to determine the level of accuracy exhibited by the proposed model. The results are contrasted with classification techniques utilizing convolutional neural networks that are rooted in deep learning principles. During the training phase, our developed model demonstrates a commendable accuracy rate of 98.82%. Subsequently, during the testing phase, the model exhibits a notable accuracy rate of 96.90%. Extensive evaluations consistently validate the superiority of the proposed paradigm over the presently employed methodology.

Index Terms- Glaucoma, Image Segmentation, U-net, Dense Net 201 Model.

I. INTRODUCTION

The The expeditious and precise diagnosis of glaucoma is of paramount importance in mitigating potential visual impairment, as emphasized by the WHO, which has reported a prevalence rate of 3.54% among individuals aged 40-80 years for this particular ailment. Glaucoma presents a notable threat to the potential loss of vision, particularly among individuals below the age of 40, wherein approximately one out of every eight individuals is susceptible to its deleterious consequences. Glaucoma is a condition characterized by elevated intraocular pressure, which has been identified as a causative factor in the pathogenesis of this disease.

The deleterious effects of this increased pressure manifest in the form of damage to optic nerves and blood vessels. Consequently, the potential consequences of glaucoma could be severe, as it may result in complete loss of vision in both eyes. This condition is often colloquially referred to as the "snake thief of sight," highlighting the insidious nature of its impact on visual function. Referred to as the "sneak disease," glaucoma is widely recognized for its initial asymptomatic nature, leading to irreversible visual impairment and holding the second position in prevalence after cataracts. Glaucoma, a prevalent ocular condition, has been identified as the cause of approximately 12% of blindness cases reported annually in the United States. Furthermore, it is anticipated that the global prevalence of glaucoma would escalate significantly, with an estimated 111.8 million individuals aged 40 to 80 being diagnosed by the year 2040. In contrast, it is noteworthy to highlight that Alzheimer's disease, which manifests with a 4.7% probability among individuals aged 70 and above, presents a comparatively diminished risk within the broader populace.

The phenomenon referred to as "retinal ganglion cell loss" (RGC) encompasses a range of processes that ultimately result in the degeneration of retinal ganglion cells. This degeneration is closely associated with impaired vision and abnormalities in both the optic nerve head (ONH) and the neocortical nerve fiber layer. When left unaddressed, glaucoma poses a significant risk to both peripheral and central vision, underscoring the importance of implementing diagnostic and therapeutic measures in the absence of a definitive cure.

Retinal fundus imaging has emerged as an essential modality for the detection and assessment of various ocular pathologies, providing a holistic evaluation of the vitreous, macula, retina, and optic nerve. By employing a fundus camera, ophthalmologists are

able to capture high-resolution images of the retina, thereby facilitating the identification and assessment of a wide range of ocular disorders. This includes glaucoma, which stands as the primary cause of visual impairment worldwide. Glaucoma-induced alterations in the central cup area of the optic nerve head (ONH) offer valuable diagnostic indicators, which could be quantified utilizing the cup-to-disc ratio (CDR). The monitoring of CDR (Cup-to-Disc Ratio) progression requires the implementation of a two-step segmentation methodology on retinal images.

The manifestation of glaucoma progression is frequently characterized by a gradual decline or complete impairment of peripheral vision. Glaucoma, a debilitating ocular condition, is renowned for its dual epithets of "the wise one" and "the thief of eyesight." This insidious disease cunningly emerges without any discernible warning signs during its initial phases, progressively culminating in irreversible blindness. The timely identification and intervention of ocular conditions play a pivotal role in enhancing the probability of maintaining visual acuity. The manifestation of glaucoma's effect on the optic cup becomes increasingly apparent as the condition progresses, leading to the phenomenon known as excavation. Elevated intraocular pressure has been observed to manifest as a luminous halo in the vicinity of intense light sources. This ocular phenomenon is associated with a spectrum of potential adverse consequences, encompassing visual impairment leading to complete loss of sight, ocular discomfort, compromised visual acuity characterized by hazy vision, and a sense of lightheadedness.

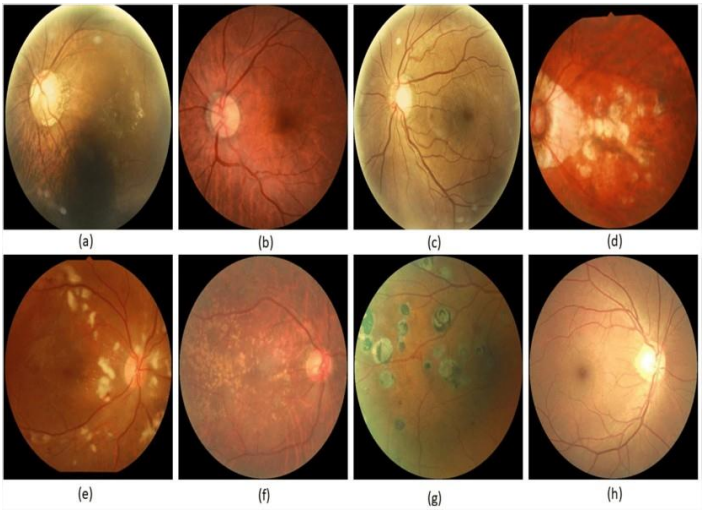

Fig. 1. Glaucoma Dataset Images or various classes

Glaucoma, a condition characterized by elevated intraocular pressure and progressive optic nerve damage, manifests in several forms, each presenting unique complexities and displaying varying frequencies across diverse racial and ethnic populations. Among these varieties are traumatic, pseudo exfoliative uveitic glaucoma, angle-closure, congenital, primary open-angle glaucoma and normal tension, a prevalent variant, is distinguished by the occurrence of optic nerve damage [5]. Figure 2 depicts the anatomical characteristics of the optic nerve head.

In the context of open-angle glaucoma, it is observed that there is a gradual accumulation of fluid pressure, which could occur even in cases where there is partial obstruction within the drainage canal. It is plausible that individuals may exhibit early detection of central vision impairment prior to the onset of peripheral symptoms, such as visual blurring, which may not be readily apparent. This phenomenon is frequently observed. Angle-closure glaucoma, alternatively referred to as acute glaucoma, manifests as a condition wherein the eye's drainage system experiences a complete failure, thereby precipitating a swift escalation in intraocular pressure and the potential for abrupt vision loss. Several factors have been identified as potential contributors to the development of this condition. These factors encompass a drooping iris and a small pupil, which collectively exert strain on the trabecular meshwork and result in the displacement of drainage channels in closer proximity to the iris. The manifestation of ocular damage could arise as a consequence of elevated intraocular pressure [6].

In the context of ocular health, it is imperative to note that the equilibrium of drainage and secretion processes plays a pivotal role. Nevertheless, it is worth noting that the obstruction of a drainage canal could potentially lead to an elevation in intraocular pressure, thereby exerting an adverse impact on the optic nerves, which play a crucial role in the transmission of visual signals to the brain. If left unmanaged, glaucoma has the potential to result in complete vision loss. Hence, the timely identification of ocular abnormalities assumes paramount importance in mitigating the risk of visual impairment. The scientific community is currently engaged in extensive investigations regarding the utilization of deep learning technologies for the purpose of early detection and prognostication of glaucoma, prior to its progression into a clinically significant condition. The utilization of a proposed deep learning model for the processing of glaucoma images involves the integration of a glaucoma dataset. The integration is accomplished by merging a deep convolutional neural network with the DenseNet-201 model, a kind of pretrained transfer learning. Utilizing this specific combination, the model's attributes and segments are derived [7]. The utilized classification technique, referred to as deep convolutional neural network (DCNN), is responsible for discerning the existence of glaucoma within the scrutinized ocular region.

Section 2 of the present study explores the existing body of research that is relevant to the topic at hand, thereby establishing a comprehensive understanding of the current state of knowledge in the field. On the other hand, Section 3 elucidates the proposed methodology, which serves as a blueprint for the systematic approach that would be employed to address the research objectives and answer the research questions. Sections 4 and 5 encompass the examination of performance and the subsequent conclusion, respectively. The present study aims to provide a comprehensive analysis of various types of glaucoma, with a particular focus on the importance of early detection utilizing advanced technologies in order to minimize the potential for vision loss.

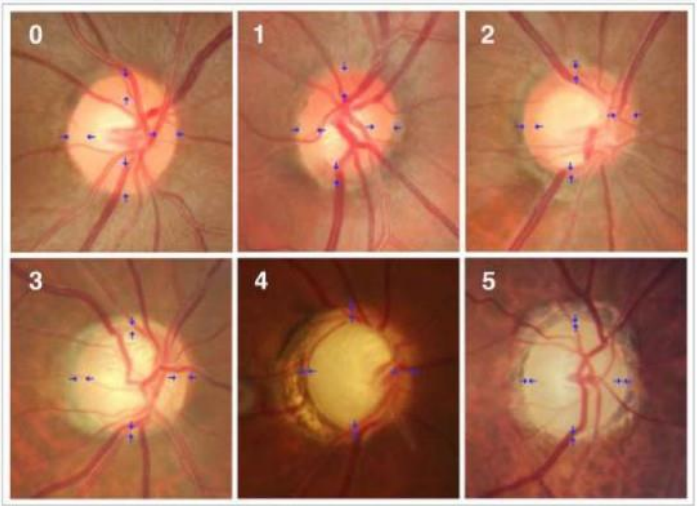

Fig. 2. The blue arrows on the optic disc images represent the different phases of glaucomatous nerve damage, which range from 0 to 5.

II. Literature Review

A multitude of models have been developed by researchers with the objective of diagnosing and categorizing glaucoma. These models encompass a wide range of research methodologies and computer programs. The collaborative endeavor has resulted in the development of numerous research frameworks, each addressing the intricate task of differentiating retinal diseases from diverse manifestations of glaucoma. The models incorporated in this study encompass a diverse array of retinal conditions, such as mild nonproliferative retinopathy, normal fundus, and macular epiretinal membrane, among other conditions [8].

Within the domain of clinical investigations, the utilization of digitally recorded retinal images has assumed a pivotal role in the identification and diagnosis of glaucoma. The diagnostic process was enhanced through the implementation of comprehensive preprocessing and segmentation techniques, thereby improving the accuracy of the results. The emergence of deep learning technologies, exemplified by U-Net and attention-based convolutional neural network (ACNN), has yielded substantial advancements in the segmentation of the optic cup. As a result, the precision of glaucoma diagnosis has been notably enhanced. The aforementioned advancements have demonstrated significant merit, as evidenced by their ability to achieve remarkably low error rates throughout the course of their implementation [13-17].

In addition to conventional approaches, a diverse range of machine learning frameworks have been investigated. Various models, including Xception, VGG-16, VGG-19, ResNet50, DeepLabv3+, MobileNet, and ensemble networks, have exhibited remarkable precision in the detection and diagnosis of glaucoma. This underscores the versatility and promising capabilities of these advanced technologies, as evidenced by multiple studies [22-27].

The incorporation of sophisticated methodologies, such as Gaussian mixture models, vector generalized gradient, principal component analysis (PCA), and support vector regression (SVR), in conjunction with deep learning methodologies like MNet and DENet, has significantly advanced the progress of glaucoma diagnostic models. The Recurrent U-Net, a well-regarded model known for its advanced segmentation techniques, has demonstrated its efficacy in the comprehensive examination of retinal fundus images. Notably, it exhibits a remarkable level of accuracy in accurately distinguishing optic disc and cup structures, as evidenced by previous studies [32-34].

Furthermore, scholars have undertaken investigations into novel methodologies, exemplified by the integration of temporal and geographical data through the utilization of recurrent neural networks (RNN). The approach presented in this study showcases encouraging results in the realm of dependable glaucoma diagnosis through the utilization of spatial and temporal information derived from fundus images [14]. The aforementioned collective advancements serve to highlight the ever-evolving nature of glaucoma diagnosis, wherein the incorporation of state-of-the-art technologies and methodologies persistently enhances the precision and effectiveness of the diagnostic procedure.

III. Methodology

Researchers recommend employing deep learning models trained on retinal fundus pictures from the Glaucoma database for glaucoma diagnosis and classification. Making utilization of Densenet-201 models that have been trained and prepared beforehand makes feature extraction much easier in this setting. The U-Net design is used to achieve the integrated segmentation procedure. Deep convolutional neural networks (DCNNs) are employed to carry out both jobs. For this investigation, the glaucoma dataset is the main source of data [17].

During the course of the Singapore Malay Eye Study (SiMES), one hundred fifty colour fundus images of the retina were acquired. These images are included in the dataset. All of the images that are included in the dataset are either images of the ground truth with the extension (.jpg) or images of the retinal fundus with the extension (.mat). Because these retinal ground truth images are now publicly available, researchers could utilize this extensive glaucoma database to test and improve their computer-aided segmentation techniques. We aim to make the glaucoma dataset publicly available online after we evaluate requests. Part of the preparation step involves carefully splitting the 650-image dataset into 488 training images and 162 test images. The steps involved in the procedure are as follows: as shown in Figure 3, convolution, down-sampling, several rounds of convolution for feature extraction, up-sampling, and finally processing through the U-Net Architecture.

One of the most popular options for medical image segmentation, the optical cup segmentation tool was built with the help of the U-Net platform's deep learning technology. Because of its thorough and efficient design, the U-Net architecture—shown in Figure 3—is frequently employed in this setting. As seen in Figure 3, deep learning is an integral part of the feature extraction process because of its capacity to maximize ROI. At the end of this procedure, the optical cup has emerged as the main structural component, which greatly affects the segmentation outcome.

In Figure 4, the processed features are input into the U-Net, and in Algorithm 1, the procedures for extracting features and

segmenting them are detailed. Throughout the planning phase, we meticulously analyzed the algorithm's capability to process the ground-truth mask png picture before disassembling it. Disc double (mask > 0) and cup double (mask > 1) equations were utilized to fabricate this mask and the optic cup (OC) mask, respectively. Following this, the OC-proximal retinal fundus area of interest was identified by utilizing the OD ground truth. The exact location of the ROI could be better understood by comparing it to the OC, which served as a reference point.

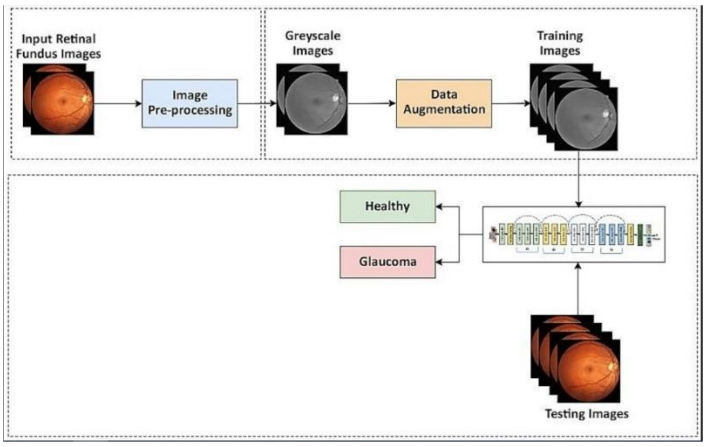

Fig. 3. U-net DL Model Architecture.

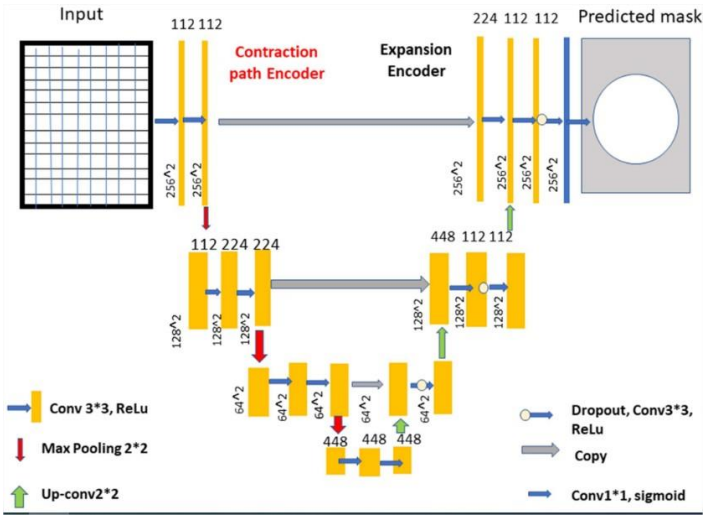

Fig. 4. Modified U-net DL Model Architecture.

When you make a left or right turn, the road narrows, but it becomes wider in the opposite way. The directional changes are coordinated by a network of interconnected lines, assisted by numerous levels of jump connections, as depicted in the middle part. The visual representations produced by these changes are subsequently directed to a layer positioned immediately after the expanding route, supervising the development of forecasts. Each convolution layer's filter banks undergo rectified linear activation after each three-padding convolution iteration, with f(z) = max(0, z) as the defining function. A set of three convolutional blocks delineates the direction of extension from that of contraction. The maximum pooling layer is applied after the contracting approach, with pool dimensions of 2 × 2 meters, after two layers of convolution. There is another convolutional layer that comes before this one.

If you want to learn more about feature extraction and segmentation, Box 1 has all the information you need. Merging and integrating two convolutional layers make up the contraction route. A dropout layer is present in both the expanding and contracting routes. A merged layer, sometimes called a dropout layer, is incorporated at this stage. There are two stages of convolutional processing that occur throughout the joining process. At the end of the process, a convolutional layer is produced that assigns a class score to every pixel. The sigmoid activation function and a single filter are utilized. After this point, no additional levels are added. In blocks 1–3, the convolution layers are set up with filter configurations of 112, 224, and 448. The counts in the expanding path and the items in the filters of blocks 5, 6, and 7 are 224, 122, and 122, respectively. Convolutional stacking involves the vertical arrangement of 448 separate filters. The suggested DCNN makes use of many filters to improve accuracy and make the most efficient use of the GPU's RAM for model storage. The model uses a DenseNet-201 and a CNN [21] and incorporates dropouts at various points in its lengthy operation. An ANN model incorporating DenseNet-201 is employed in this trial. In order to correctly recognize retinal fundus images and identify glaucoma cases in the input dataset, the DenseNet-201 model employs deep transfer learning.

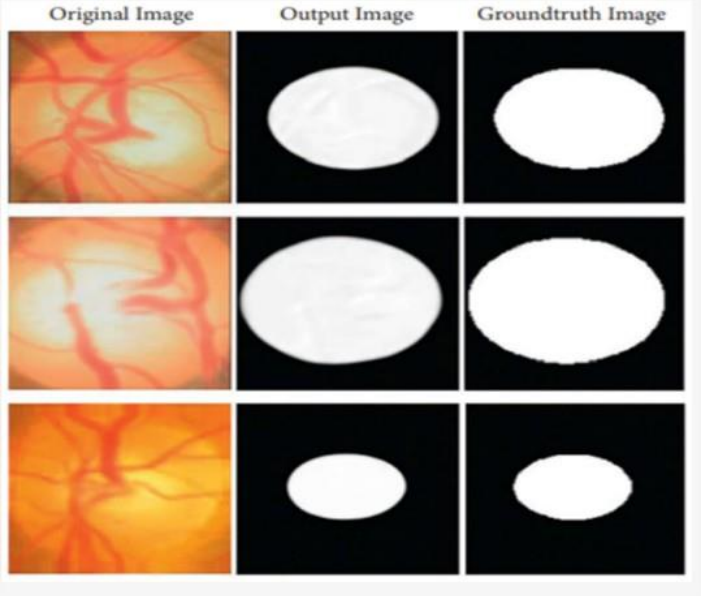

Fig. 5. Original image & ground truth images

The approach utilized comprises utilizing a pretrained DenseNet-201 model to extract features from the dataset. Then, a Deep Convolutional Neural Network (DCNN) model is employed to categorize the data. The input images being processed have a defined resolution of 256 by 256 pixels. Figure 5 visually illustrates the architecture of the DCNN, which includes DenseNet-201. This architecture demonstrates the complex

arrangement and interconnections inside the model, highlighting the framework utilized for the efficient processing and categorization of the input data.

Transfer Learning (TL) could be beneficial in Convolutional Neural Network (CNN) applications when the amount of collected data is limited. Transfer learning utilizes the knowledge acquired from large datasets, like ImageNet, to improve the performance of applications that have smaller datasets. By circumventing the requirement for a large volume of training data, deep learning algorithms become more versatile and may be applied to a wide range of applications. The concept entails training a model for a certain task and then utilizing it to train another model for a similar task. This approach optimizes the transfer learning network and reduces the time and computational resources required, as opposed to developing the second model from the beginning. Utilizing pretrained models, especially those trained on extensive datasets, allows for training new models on smaller labeled datasets, resulting in reduced training time and processing requirements. The DenseNet-201 model is distinguished by its compact network structure, which improves performance by creating highly parameterized, efficient, and easily trainable models. DenseNet-201 exhibits outstanding performance on datasets like as ImageNet and CIFAR-100. It achieves this by incorporating direct connections that connect each layer to the next, resulting in enhanced connectivity. This could be seen in Figure 5. The design utilizes dense blocks to perform down-sampling, which includes transition layers and 1-1 convolution layers. This enhances the model's capacity to adapt to different environmental situations.

The DenseNet-201 model utilizes a growth rate, represented by the "H" hyper-parameter, which determines how the dense design improves performance. Although the growth rate is not significant, the architecture stands out because of its feature maps that depict the overall state of the network, allowing each layer to access the function mappings from the preceding layers. The input feature mappings at each layer, represented as "fm," are computed, and each 3 × 3 convolution layer is accompanied by an extra 1 × 1 convolution layer, which serves as a "bottleneck." During the process of classification, the fully connected (FC) layers serve as classifiers by converting 2D feature maps into 1D feature vectors. Activation functions and dropout layers incorporate nonlinearity and mitigate overfitting. In order to improve accuracy, a sigmoid activation function is utilized before the final fully connected (FC) layer in DenseNet-201 for binary classification. In this case, the sigmoid function is mathematically defined as S = (1/(1 + e(-xz))), where S represents the output of the neuron, and xi and zi represent the inputs and weights, respectively. Applying the sigmoid function to categorize images according to their glaucoma risk is a rational approach, as it yields binary outputs of either 0 or 1. Dropout methods are employed to mitigate overfitting in the early fully connected (FC) layers, while the sigmoid activation function guarantees that the classification output remains within the normalized range. Figure 6 demonstrates the operating concepts of the DenseNet-201 design, highlighting its complex architecture and functionality.

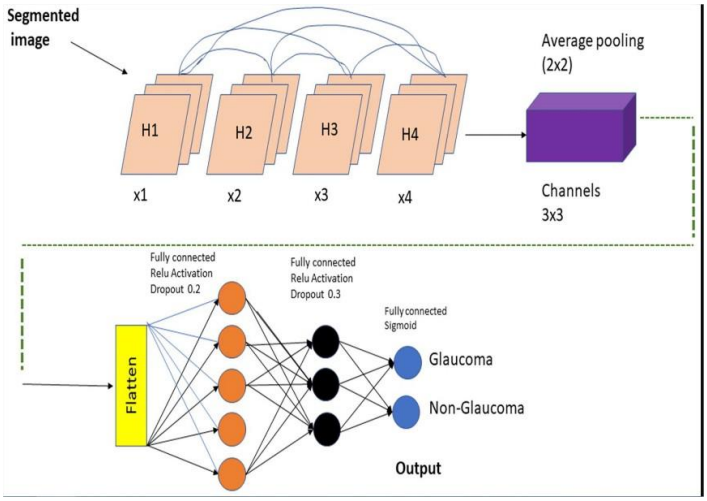

Fig. 6. Classification with DCNN and feature extraction with a pretrained DenseNet-201 model

IV. RESULTS

This dataset evaluates the performance of the DCNN, U-Net, and DenseNet-201 models. When assessing a model, the F-measure, accuracy, precision, recall, and specificity are all taken into account. By comparing research, one may further validate the technique. Currently, powerful deep learning models like ResNet, DenseNet-169, ResNet 152v4, and VGG-19 are being employed to assess the results of CNN classification. Every Python test utilizes a training set including just 33.33% of the data, while the remaining 66.67% is reserved for performance analysis.

The main objective of this research project is to diagnose glaucoma and evaluate its effects on individuals. The model's output could vary between positive and negative results based on its ability to accurately detect the presence of glaucoma. By employing this approach, individuals could acquire an initial understanding of the potential results by examining specific positive and negative outcomes, along with any other possible possibilities, regardless of their likelihood. Put simply, it displays the overall count of accurate predictions. The term "FP" represents the count of accurately predicted and observed positive outcomes. Upon encountering this numerical value, you would gain understanding of the frequency with which you accurately adhered to a particular course of action. If there is a failure, this function calculates the overall count of inaccurate projections. The accuracy of a model pertains to its capacity to precisely predict the behaviours of a specific cohort. The utilization of it in the classification process influences the level of efficiency. The objective is to offer a comprehensive understanding of the frequency at which both positive and negative classes are needed. The categorization of glaucoma fundus images demonstrated that the utilization of the suggested model for training and testing resulted in superior accuracy compared to previous approaches. The results of this investigation are presented in Table 1 and Figure 7. Compared to earlier methods, it demonstrated an average improvement in training accuracy ranging from 1.09% to 3.96%. The tests exhibit a 96.90% accuracy rate in comparison to the alternative models being evaluated, indicating a performance enhancement ranging from 1.36% to 5.26%.

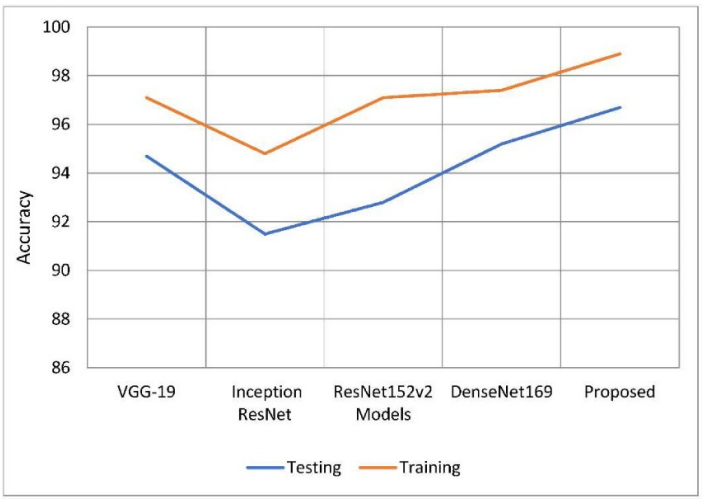

Fig. 7. Comparison of pre-trained model accuracy with developed methodology

Table 1. Models Accuracy

DL Models	Training	Testing
VGG-19	97.73	95.54
ResNet 152v2	97.56	93.21
Inception ResNet	94.86	91.64
U-Net	98.11	96.37
DenseNet169	97.14	95.45
Proposed Model	98.82	96.90

The accuracy of outcomes depends on accurate forecasts, which, in turn, assesses the probability of receiving a favorable comment. An evaluation is conducted utilizing the already accessible data to ascertain the expected precision of the outcomes. A decline in accuracy has led to an increase in the number of false positive predictions produced by the categorization model. Table 2 and Figure 8 demonstrate the higher accuracy of the suggested model compared to the models utilized for comparison. The training accuracy of the model is 98.63%, which is an improvement of 1.1 to 4.8% compared to other methodologies. Moreover, the model exhibits an accuracy rate of 96.45%, surpassing other models by a performance improvement ranging from 1.08% to 4.9%.

Two perspectives on precision analysis are shown in Figure 7, and "recall" and "sensitivity" could be employed interchangeably in some contexts. When calculating the positive predictive value, the "positive predictive value ratio" measures how much of that value might be attributed to accurate forecasts. The classification model appears to be significantly impacted by false negative discoveries, according to the recall value of the model. Recall is enhanced when the ratio of the known and recalled information is divided by the total information that has to be remembered.

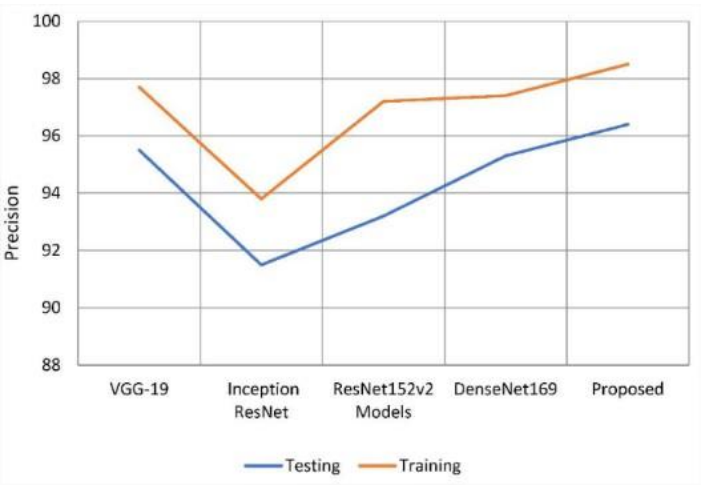

Fig. 8. Comparison of pre-trained model precision with developed methodology

Table 1. Models Precision

Models	Training	Testing
Inception ResNet	93.81	91.52
VGG-19	97.30	94.70
DenseNet169	97.49	95.37
ResNet 152v2	97.28	93.02
U-Net	98.02	95.97
Proposed Model	98.63	96.45

According to the data in Table 3and 4, the suggested model exhibits dominant sensitivity and recall compared to previous models.

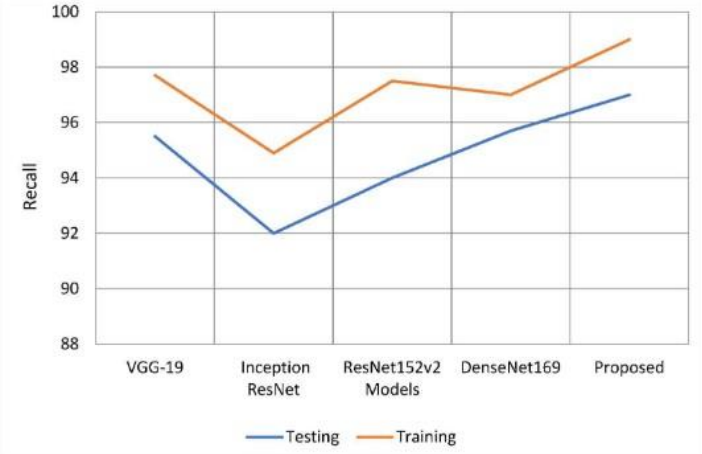

Fig. 9. Comparison of pre-trained model Recall with developed methodology

The recall rates demonstrated a range of improvement, varying from 1.1% to 4.05 %, in comparison to previous methods. Based

on the analysis, the rate of product recalls exceeded that of other models by a margin ranging from 1.3 to 5.06% points. The differences in performance are vividly illustrated in Figure 9.
The measure of a model's accuracy in predicting the probability of infection in a healthy individual is referred to as "specificity." This refers to the overall count of persons whose samples were analyzed and found to be devoid of the specific disease being investigated. The suggested model demonstrated superior specificity rates in comparison to previous deep learning models, with a specificity rating of 98.15%. By comparison, previous methods only attained specificity scores ranging from 0.8 to 4%. The significant enhancement is seen in Figure 10, which presents a comparison of the estimated specificity values.

The F-measure, which is calculated as the weighted harmonic mean of accuracy and recall, provides a comprehensive tool for evaluating the precision of a diagnostic model. It guarantees precise control and administration of the distribution of the dataset, especially when handling imbalanced categories. The proposed model demonstrated superior performance compared to other models, with an enhanced F-measure training success rate of 98.50 % to 3.7%. Throughout the testing phase, the suggested model demonstrated superior F-measure rates, outperforming competing models by a margin ranging from 0.08 % to 4.47%. The suggested model exhibited exceptional performance in both the training and testing phases, surpassing earlier models in multiple dimensions.

The U-Net model, employed for segmentation tasks, provides benefits over earlier methods by effectively incorporating both global location and context information. The addition of higher-resolution feature maps from the encoder network in its unique design enables enhanced representation learning. The U-Net model employs parallel dilated convolution to improve its semantic segmentation performance, allowing for the utilization of deeper networks while maintaining efficient feature extraction. This study highlights the benefits of the provided network model and its new structural aspects in obtaining excellent performance in segmentation-related tasks, even with a small number of training data.

V. DISCUSSION

The global prevalence of glaucoma, which currently affects over 78 million people, is projected to increase to 111.8 million cases by 2040. Researchers propose the utilization of deep learning techniques for the detection and prediction of glaucoma. High intraocular pressure, considered a primary factor in the development of glaucoma, is hypothesized to cause damage to the blood vessels and neurons in the eye. Known as the "sneak disease," glaucoma frequently appears without obvious symptoms, although a significant sign is the gradual loss of peripheral vision. Potential consequences include loss of sight, eye irritation, reduced visual acuity, severe nausea, and vertigo. Early detection and prompt treatment improve the chances of preserving eyesight in the damaged eye. Elevated intraocular pressure could exert pressure on the trabecular meshwork, which may result in the obstruction of drainage channels in close proximity to the iris.

In order to detect and predict the occurrence of glaucoma, experts recommend utilizing deep learning models that have been particularly trained on retinal fundus images obtained from the glaucoma database. The U-Net platform, which employs deep learning technology, plays a crucial role in developing an optical cup segmentation tool. The segmentation result is greatly affected by the technique of extracting minor features. The study employed a DenseNet-201 model to extract features and a DCNN model for categorizing data. The dataset is divided into 162 test images and 488 training images after preprocessing.

Convolutional stacking incorporates 448 filters in the course of the operation. Transfer learning utilizes the knowledge acquired from extensive datasets such as ImageNet to improve the performance of applications that have comparatively smaller datasets. This approach helps to decrease the time and computational resources required for training. Additional 1×1 convolution layers are included in each 3×3 convolution layer to speed up processing. Classifiers in the classification phase are fully connected (FC) layers. To counteract the risk of overfitting due to non-normalized input data, the earliest FC layers utilizes dropout to ensure that neurons do not fire randomly. Depending on whether glaucoma is present, the U-Net model generates positive or negative results. When compared to previous methods, the model's accuracy—as judged by its subset behavior prediction abilities—increased training accuracy by 1.09 to 3.96%. Nevertheless, a decrease in precision resulted in a higher count of incorrect positive forecasts in the classification model. However, the proposed model exhibited higher accuracy than the comparator models, as evidenced by the recall value which indicated a reduction in false negatives in the categorization model.

VI. CONCLUSION

This study raises the possibility of utilizing deep learning as an innovative approach to glaucoma diagnosis and prognosis. Employing the glaucoma dataset, the researchers trained a deep learning network to identify the disease in images. The majority of the dataset was reserved for instructional training, while a tiny fraction (less than a quarter) was set aside for study. Data separation was accomplished with the help of the U-Net segmentation model, and feature extraction was carried out by DenseNet-201, a pretrained transfer learning model that makes utilization of a DCNN. By training a deep convolutional neural network to categorize retinal fundus images, glaucoma was successfully identified. This study set out to analyze retinal fundus images in order to detect glaucoma in humans. Following the optic cup region extraction from fundus images, the ground truth images in the dataset were compared to the generated image data. The DenseNet model played a crucial role in extracting features from segmented images for the purpose of organizing the data. The evaluation findings indicated that the model attained a testing accuracy of 96.90% and a training accuracy of 98.82%, outperforming other models by a margin of 1.36% to 5.26%. Both comparing and training analyses highlighted the model's exceptional accuracy compared to other approaches.

The model's conclusions from the performance investigation could be deemed accurate, albeit a minor discrepancy (98.4% accuracy)

was seen due to prevailing findings. It is expected that the classifier's performance would increase and the threshold would be lowered to fix this mismatch. The presented methodologies shown the capability to detect diverse medical ailments including breast cancer, brain tumors, and diabetic retinopathy. This paper contains a thorough documentation of the methodology and insights gained from future reviews. The experimental results demonstrated the higher performance of the DenseNet-201-D approach compared to other current technologies. Potential future directions for research include developing a range of DenseNet-based deep neural networks with different transfer learning settings. Furthermore, there is a need to better investigate the identification of lesions associated with multiple sclerosis (MS) in neuroradiology diagnostic work. Manufacturing, transportation engineering, and industrial imaging are just a few examples of the numerous non-medical fields that could benefit from the suggested transfer learning strategy, which is based on the results of this study. Research into fuzzy and semi-supervised methods would continue in the future.

REFERENCES

[1] Senjam, S. Glaucoma blindness–A rapidly emerging non-communicable ocular disease in India: Addressing the issue with advocacy. J. Fam. Med. Prim. Care 2020, 9, 2200.

[2] Kumar, B.N.; Chauhan, R.P.; Dahiya, N. Detection of glaucoma using image processing techniques: A review. In Proceedings of the 2016 International Conference on Microelectronics, Computing and Communications (MicroCom), Durgapur, India, 1–9 January 2016.

[3] Barros, D.M.S.; Moura, J.C.C.; Freire, C.R.; Taleb, A.C.; Valentim, R.A.M.; Morais, P.S.G. Machine learning applied to retinal image processing for glaucoma detection: Review and perspective. BioMed. Eng. Online 2019, 19, 20.

[4] Li, L.; Xu, M.; Liu, H.; Li, Y.; Wang, X.; Jiang, L.; Wang, Z.; Fan, X.; Wang, N. A large-scale database and a CNN model for attention-based glaucoma detection. IEEE Trans. Med. Imaging 2020, 39, 413–424.

[5] Wang, Y.; Panda-Jonas, S.; Jonas, J. Optic nerve head anatomy in myopia and glaucoma, including parapapillary zones alpha, beta, gamma and delta: Histology and clinical features. Prog. Retin. Eye Res. 2021, 83, 100933.

[6]

[7] Juneja, M.; Singh, S.; Agarwal, N.; Bali, S.; Gupta, S.; Thakur, N.; Jindal, P. Automated detection of Glaucoma using deep learning convolution network (G-net). Multimed. Tools Appl. 2020, 79, 15531–15553.

[8] Diaz-Pinto, A.; Morales, S.; Naranjo, V.; Köhler, T.; Jose, M.; Navea, A. CNNs for automatic glaucoma assessment using fundus images: An extensive validation. BioMed. Eng. Online 2019, 18, 29.

[9] Fu, H.; Cheng, J.; Xu, Y.; Liu, J. Glaucoma detection based on deep learning network in fundus image. In Deep Learning and Convolutional Neural Networks for Medical Imaging and Clinical Informatics, Advances in Computer Vision and Pattern Recognition; Lu, L., Wang, X., Carneiro, G., Yang, L., Eds.; Springer: Cham, Switzerland, 2019; pp. 119–137.

[10] Jiang, Y.; Wang, F.; Gao, J.; Cao, S. Multi-path recurrent U-Net segmentation of retinal fundus image. Appl. Sci. 2020, 10, 3777.

[11] Mahum, R.; Rehman, S.U.; Okon, O.D.; Alabrah, A.; Meraj, T.; Rauf, H.T. A novel hybrid approach based on deep CNN to detect glaucoma using fundus imaging. Electronics 2022, 11, 26.

[12] Glaucoma_Dataset. Kaggle.com. 2022. Available online: https://www.kaggle.com/datasets/sreeharims/glaucoma-dataset (accessed on 2 July 2022)

[13] Yasir, E.A.M.; Bashir, H.I. Classification of diabetic retinopathy using stacked autoencoder-based deep neural network. J. Comput. Sci. Intell. Technol. 2020, 1, 9–14.

[14] Narmatha, C.; Hayam, A.; Qasem, A.H. An analysis of deep learning techniques in neuroimaging. J. Comput. Sci. Intell. Technol. 2021, 2, 7–13.

[15] Manimegalai, P.; Jayalakshmi, P.K. A study on diabetic retinopathy detection using image processing. J. Comput. Sci. Intell. Technol. 2021, 2, 21–26.

[16] Jaiswal, A.; Gianchandani, N.; Singh, D.; Kumar, V.; Kaur, M. Classification of the COVID-19 infected patients using DenseNet201 based deep transfer learning. J. Biomol. Struct. Dyn. 2020, 39, 5682–5689.

[17] Nair, R.; Bhagat, A. An Introduction to Clustering Algorithms in Big Data. In Encyclopedia of Information Science and Technology, 5th ed.; IGI Global: Hershey, PA, USA, 2021; pp. 559–576.

[18] Nair, R.; Zafrullah, S.N.; Vinayasree, P.; Singh, P.; Zahra, M.M.A.; Sharma, T.; Ahmadi, F. Blockchain-Based Decentralized Cloud Solutions for Data Transfer. Comput. Intell. Neurosci. 2022, 2022, 8209854.

[19] Kashyap, R. Applications of Wireless Sensor Networks in Healthcare. In Advances in Wireless Technologies and Telecommunication; IGI Global: Hershey, PA, USA, 2020; pp. 8–40.

[20] Nair, R.; Gupta, S.; Soni, M.; Shukla, P.K.; Dhiman, G. An approach to minimize the energy consumption during blockchain transaction. Mater. Today Proc. 2020; in press.

[21] Waoo, N.; Kashyap, R.; Jaiswal, A. DNA Nano array analysis using hierarchical quality threshold clustering. In Proceedings of the 2010 2nd IEEE International Conference on Information Management and Engineering, Chengdu, China, 16–18 April 2010; pp. 81–85.

[22] Kashyap, R. Big Data Analytics Challenges and Solutions. In Big Data Analytics for Intelligent Healthcare Management; IGI Global: Hershey, PA, USA, 2019; pp. 19–41.

[23] Naseri, M.; Abdolmaleky, M.; Laref, A.; Parandin, F.; Celik, T.; Farouk, A.; Mohamadi, M.; Jalalian, H. A new cryptography algorithm for quantum images. Optik 2018, 171, 947–959.

[24] Krishnamoorthi, R.; Joshi, S.; Almarzouki, H.Z.; Shukla, P.K.; Rizwan, A.; Kalpana, C.; Tiwari, B. A Novel Diabetes Healthcare Disease Prediction Framework Using Machine Learning Techniques. J. Healthc. Eng. 2022, 2022, 1684017.

[25] Ahmad, I.; Serbaya, S.H.; Rizwan, A.; Mehmood, M.S. Spectroscopic analysis for harnessing the quality and potential of gemstones for small and medium-sized enterprises (SMEs). J. Spectrosc. 2021, 2021, 6629640.

[26] Mary, M.C.V.S.; Rajsingh, E.B.; Naik, G.R. Retinal fundus image analysis for diagnosis of glaucoma: A comprehensive survey. IEEE Access 2016, 4, 4327–4354.

[27] Sarhan, A.; Rokne, J.; Alhajj, R. Glaucoma detection using image processing techniques: A literature review. Comput. Med. Imaging Graph. Off. J. Comput. Med. Imaging Soc. 2019, 78, 101657.

[28] Prastyo, P.H.; Sumi, A.S.; Nuraini, A. Optic cup segmentation using U-Net architecture on retinal fundus image. J. Inf. Technol. Comput. Eng. 2020, 4, 105–109.

[29] MacCormick, I.J.C.; Williams, B.M.; Zheng, Y.; Li, K.; Al-Bander, B.; Czanner, S.; Cheeseman, R.; Willoughby, C.E.; Brown, E.N.; Spaeth, G.L.; et al. Accurate, fast, data efficient and interpretable glaucoma diagnosis with automated spatial analysis of the whole cup to disc profile. PLoS ONE 2019, 14, e0209409

[30] SynaSreng, N.M.; Hamamoto, K.; Win, K.Y. Deep learning for optic disc segmentation and glaucoma diagnosis on retinal images. Appl. Sci. 2020, 10, 4916.

[31] Gheisari, S.; Shariflou, S.; Phu, J.; Agar, A.; Kalloniatis, M.; Golzan, S.M. A combined convolutional and recurrent neural network for enhanced glaucoma detection. Sci. Rep. 2021, 11, 1945.

[32] Nair, R.; Bhagat, A. An Application of Big Data Analytics in Road Transportation. In Advances in Systems Analysis, Software Engineering, and High Performance Computing; IGI Global: Hershey, PA, USA, 2018; pp. 39–54.

[33] Kashyap, R.; Piersson, A. Big Data Challenges and Solutions in the Medical Industries. In Advances in Systems Analysis, Software Engineering, and High Performance Computing; IGI Global: Hershey, PA, USA, 2018; pp. 1–24.

[34] Almarzouki, H.Z.; Alsulami, H.; Rizwan, A.; Basingab, M.S.; Bukhari, H.; Shabaz, M. An Internet of Medical Things-Based Model for Real-Time Monitoring and Averting Stroke Sensors. J. Healthc. Eng. 2021, 2021, 1233166.

[35] Heidari, S.; Abutalib, M.M.; Alkhambashi, M.; Farouk, A.; Naser, M. A new general model for quantum image histogram (QIH). Quantum Inf. Process. 2019, 18, 175.

AUTHORS

Syed Bacha Hussain Bukhari holds a Bachelor's in Mechatronics Engineering from the University of Engineering and Technology, Peshawar. Currently pursuing a Master's with a focus on Automation and Control, Syed Bacha Hussain Bukhari works as an Instrumentation and Control Engineer at CCCL, combining academic expertise with practical experience.

Dr. Shahzad Anwar is currently working as Associate Professor at Department of Mechatronics Engineering and Principal Investigator at Artificial Intelligence in Healthcare, National Center of AI, UET Peshawar, Pakistan.

Correspondence Author – Syed Bacha Hussain Bukhari